Solar rotary kiln for continuous treatment of particle material: Chemical experiments from micro to milli meter particle size

Cite as: AIP Conference Proceedings **2303**, 140007 (2020); https://doi.org/10.1063/5.0029271
Published Online: 11 December 2020

Stefania Tescari, Pradeepkumar Sundarraj, Gkiokchan Moumin, Juan Pablo Rincon Duarte, Christos Agrafiotis, Lamark de Oliveira, Christian Willsch, Martin Roeb, and Christian Sattler

Solar Rotary Kiln for Continuous Treatment of Particle Material: Chemical Experiments from Micro to Milli Meter Particle Size

Stefania Tescari[1, a)], Pradeepkumar Sundarraj[1], Gkiokchan Moumin[1,2], Juan Pablo Rincon Duarte[1,2], Christos Agrafiotis[1], Lamark de Oliveira[1], Christian Willsch[1], Martin Roeb[1], Christian Sattler[1,2]

[1]*German Aerospace Center (DLR), Institute of Solar Research, Linder Hoehe, Cologne 51147, Germany*
[2]*TU Dresden, Faculty of Mechanical Science and Engineering, Institute of Power Engineering, Solar Fuel production, 01062 Dresden, Germany*

[a)]Corresponding author: Stefania.Tescari@dlr.de

Abstract. Rotary kilns are very robust and versatile reactors and can be used on solar towers to perform high-temperature endothermic thermal decomposition reactions of solid materials with the aid of concentrated solar irradiation. Their easy functioning system allows flexibility with respect to a wide range of operating conditions, such as particle size, residence time, operating temperature, furnace atmosphere etc. In the present study, two different solid materials with different particle sizes are successfully treated to demonstrate the versatility of this reactor: redox oxide granules of mm size are thermally reduced for high temperature thermochemical storage and micrometric particles of $CaCO_3$ are calcined to produce lime (as the main ingredient of cement). Preliminary tests for using the rotary kiln in thermochemical storage were carried out in a closed-chamber configuration, where the reactor atmosphere is separated from the environment. The increase in the oxygen concentration in the outlet gas could clearly indicate the onset and progress of chemical reaction. The increase in residence time has been identified as the key point for increasing the conversion of the solid material. Calcination of $CaCO_3$ was demonstrated in 13 chemical experiments. The heat losses mechanisms have been studied and pointed out that the suction of gas should be optimized to increase the efficiency of the reactor. It has also been shown that the reactor efficiency can be increased by reducing the material conversion. Optimal operation therefore depends on the final target application.

INTRODUCTION

Concentrated solar energy can provide high temperature renewable heat. This makes it an attractive candidate not only for electricity production, but also for other high-temperature industrial processes. An example is the production of lime or phosphate, where a large amount of energy is used to heat a solid material in the form of particles at temperatures close to 1000 °C. In these processes, the starting material is pre-processed in a crusher and has a wide particle size distribution (PSD). A precisely sized material would require further treatment and a consequent increase in price as well as in the quantity of waste material. The PSD can often vary over three or more orders of magnitude, from the micrometer to the millimeter scale. Therefore the treatment of this material requires a very robust, yet flexible reactor. In the past, several solar reactors have been proposed for particle treatment, such as fluidised bed, vortex or entrained flow reactors, but these concepts only work with a narrow PSD. On the contrary, the rotary kiln can work with a wide range of particles.

The introduction of concentrated solar energy in rotary kilns is not a new subject. Already in the 50s, Trombe and Foex [1] proposed such a reactor for the thermal treatment of various materials, such as the purification of alumina and quartz. Since then, a broad variety of applications have been carried out in solar rotary kilns. Examples are the decarbonation of $CaCO_3$ [2], the solar recycling of aluminum scrap [3-5], the melting of salts such as Na_2SO_4

SolarPACES 2019
AIP Conf. Proc. 2303, 140007-1–140007-8; https://doi.org/10.1063/5.0029271
Published by AIP Publishing. 978-0-7354-4037-1/$30.00

[6], or the reduction of zinc oxide for thermochemical production of hydrogen [7, 8]. However, until now, most of those experimental reactors could treat a few hundred grams per hour of particles with a narrow PSD.

In the present study two different applications with very different particle sizes are chosen and demonstrated experimentally. Both applications take place in air and at temperatures close to 1000°C. The versatility of such a reactor is thus demonstrated at a scale of 10 kg/h.

The first application (application 1) is thermochemical storage of solar heat through thermal reduction of metal oxide granules. During the hours of high solar radiation, the granules (storage medium) are heated and a reversible endothermic reaction takes place (storage charge). During cloud passage or during the night, the storage can be discharged by releasing the heat of the exothermic reverse reaction plus some of the sensible heat. The literature presents two rotary kilns with a similar objective. The first one was developed to cyclically reduce and oxidize cobalt oxide powder (Co_3O_4/CoO) [9]. In a typical test, a batch of 200 g of Co_3O_4 powder (average diameter of 10µm) was cycled between 1000 °C and 750 °C to complete the reduction and oxidation of the material respectively. A second case is based on the CuO/Cu_2O cycle, with particles smaller than 10µm. A batch of 10 g of CuO powder was heated to 850 °C to allow reduction of the metal oxide [10, 11]. Both reactors operated in batch mode, i.e. oxidation and reduction take place in the same reactor. The switch from one to the other reaction mode is realized by changing the temperature of the entire system. This lowers the reactor efficiency due to the high thermal inertia of the reactor compared to the particles batch. In the present study, the reactor operates continuously, so that the system is heated only at start-up, and then is kept at constant temperature, while the particles are heated up by flowing through it. Moreover, the quantity of material treated is higher in this study.

The second application (application 2) of this study is the decarbonation of $CaCO_3$ to produce lime (as the main ingredient of cement). Some experiments have already been carried out on this subject. In the 1980s, a small rotary kiln was tested with $CaCO_3$ particles between 200 and 300 microns in size and with an operating temperature of about 1000°. The reactor was able to treat about 300g/h. A second continuous rotary kiln was developed a few years later. The system was able to treat up to 3 kg/h of particles at temperatures of 1050-1150 °C. The particle size varied between 1-5 mm [12]. An indirect concept of a multi-tubular rotary kiln was developed and tested by the same group [13, 14]. This time the particles were not heated directly by the incident radiation but the radiation entered a cavity and heated the surface of the tubes, which transferred heat to the particles. The 1-5 mm diameter particles were fed at a rate of 2-8 kg/h and heated up to 950-1150 °C. In the present study a directly irradiated concept is considered, which allows treating particles with dimensions between 1-200µm, more suitable for industrial application.

REACTOR DESIGN

The rotary kiln, shown in Fig. 1, consists of a rotating part (drawn in blue) and a static part (in grey). The reactor core is a cylindrical inconel crucible 0.24 m in diameter and 0.7 m in length. Parallel to the axis, eight strips 1 mm high are welded along the length to improve particle mixing. The crucible is surrounded by a high-temperature blanket-shaped insulation with a thermal conductivity of 0.04 W/m·K at 800°C. The insulation is covered by an aluminum outer housing with two circular rings in contact with the four wheels to ensure smooth rotation. The rotation is driven by a motor connected by a chain to a toothed wheel fixed on the rotating body. The rotation speed can be adjusted from 0 to 10 rpm.

The particles are fed into the reactor via a screw feeder; their flow rate can be adjusted between 0 and 65 kg/h, depending on the screw speed and material properties. The dosing tube has a diameter of 30 mm and is equipped with an external water cooling system, to ensure a temperature of less than 50°C to the motor. For the brittle millimetric granules of metal oxide (application 1) a screw with an external diameter of 19 mm is used to reduce the mechanical stress on the particles. For the micrometric and cohesive particles of cement raw meal (CRM) (application 2) a screw with an external diameter of 25 mm is preferred, to reduce the compaction of the particles around the screw.

The complete system is mounted on an aluminium supporting structure, where the inclination can be adjusted from 0 to 6.5° through a hydraulic cylinder. In a typical experiment the rotation speed has been set to 2-4 rpm and the inclination to about 1°. This allows the particles to flow through the crucible in about 4 minutes.

A non-rotating front part allows the extraction of the particles and the entry of the incident radiation. A system with two conical flanges separates the reactor aperture from the particle flow zone. Between the front and the rotating part is the particle extraction system, consisting of a hopper, a pipe and a storage container. All these components are insulated through high-temperature insulation.

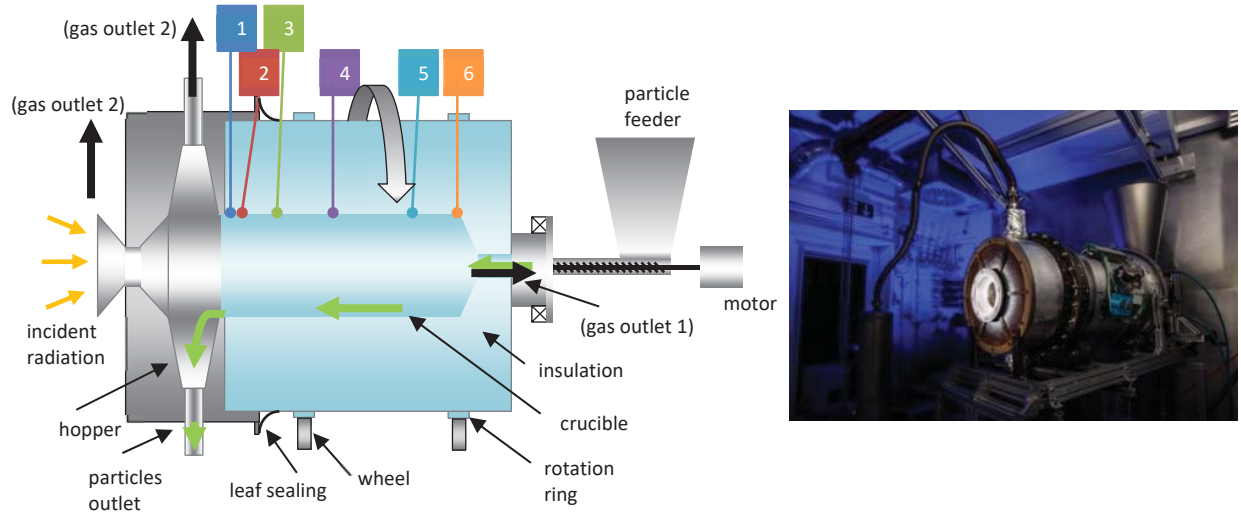

FIGURE 1. a) Diagram of the rotary kiln, with rotating parts (blue) and fixed parts (grey). From right: screw feeder, insulated rotating crucible, fixed front panel. The green arrows show the direction of particles flow. The thick black arrows represent the gas flow in closed (gas outlet 1) and open (gas outlet 2) configuration. The coloured squares numbered from 1 to 6 show the position of the thermocouples along the kiln. b) Photograph of actual reactor during operation

The system can operate both in a closed and open configuration. In the closed configuration, a quartz window is placed at the aperture where the radiation passes. The gas suction unit is applied to the back of the reactor (gas outlet 1 in Fig.1). In the open configuration, the window is removed and two suction units are applied at the front and at the aperture (gas outlet 2), to prevent the escape of particles. In both configurations the outlet gas temperature is reduced in a water cooling unit, filtered of any fine particles and sucked in by a blower. The typical gas flow is about 80 slm in closed configuration and 500 slm in open configuration. An oxygen sensor placed after the filter analyses the composition of the gas to monitor the reaction advancement. The temperatures at various points along the reactor are measured through a series of eight thermocouples, six connected to the outer wall of the crucible and two on the outer housing. The reactor has been iteratively improved over several experimental campaign and several problems were solved [15, 16].

The incident power is provided by a high flux solar simulator [17] consisting of 10 short-arc xenon lamps with elliptical reflectors. The short wavelength radiation produced by the lamps is concentrated at a focal spot at a distance of about 3 m, where the reactor aperture is located. In the current configuration, a power of 14 kW enters through the aperture of 8 cm, with a peak flux of 4000 kW/m².

APPLICATIONS

Thermochemical Storage

The first application of the solar rotary kiln is the thermochemical storage for solar power plants, based on metal oxide redox reactions. These materials store and release thermal energy by absorbing and releasing oxygen at temperatures between 350 °C and 1100 °C [18]. A specific advantage of these systems is the use of air both as a heat transfer medium and reactant, eliminating the need for heat exchangers or gas storage tanks. This makes them highly suitable option for air-operated solar plants.

Several metal oxides have been proposed as storage media [19-21]. Cobalt oxides have shown high energy density and good cyclability, but on the other hand the material is expensive and correlated with health concern issues [22-24]. On the contrary, Mn oxides are less expensive and not dangerous, but significant degradation after several cycles can be an important adverse issue [25].

Carrillo [26] has shown that the addition of Fe_2O_3 to the Mn-oxide could decrease its cycle-to-cycle degradation. This mixed oxide was therefore chosen as storage material in the present study, with a ratio of $(0.7{\cdot}Mn_2O_3)(0.3{\cdot}Fe_2O_3)$. This composition has been shown to be suitable due to cyclability, operating temperature and reaction enthalpy [19, 27]. The endothermic reaction is the reduction of the mixed metal oxide:

$$3(Mn,Fe)_2O_3 \rightarrow 2(Mn,Fe)_3O_4 + 1/2\ O_2 \quad (1)$$

The material has been shaped into 1-2 mm diameter granules to facilitate handling. It is thermally reduced at about 1050 °C inside the solar rotary kiln described above. In the same project, the storage discharge was studied through a moving bed reactor [28], which could be coupled to the rotary kiln. A techno-economic analysis on a commercial scale shows the potential of the complete system [29].

This work focuses on the reduction reaction inside the solar rotary kiln operating in a closed configuration. Two high temperature seals have been added between the rotating and the stationary part, a leaf seal between the front and rotating housing and a smaller seal between the rotating housing and the feeding unit. The reactor aperture was covered by a 25 cm diameter quartz window. The suction unit (gas outlet 1 in Fig. 1 a), applied to the back of the reactor, prevents any deposition on the window. Any fine particles, created by the abrasion of the granules in the kiln or in the feeder are entrained with the gas flow and captured in the filter. The oxygen sensor is connected to the suction unit to monitor the reaction advancement. An example of the results is shown in Fig. 2.

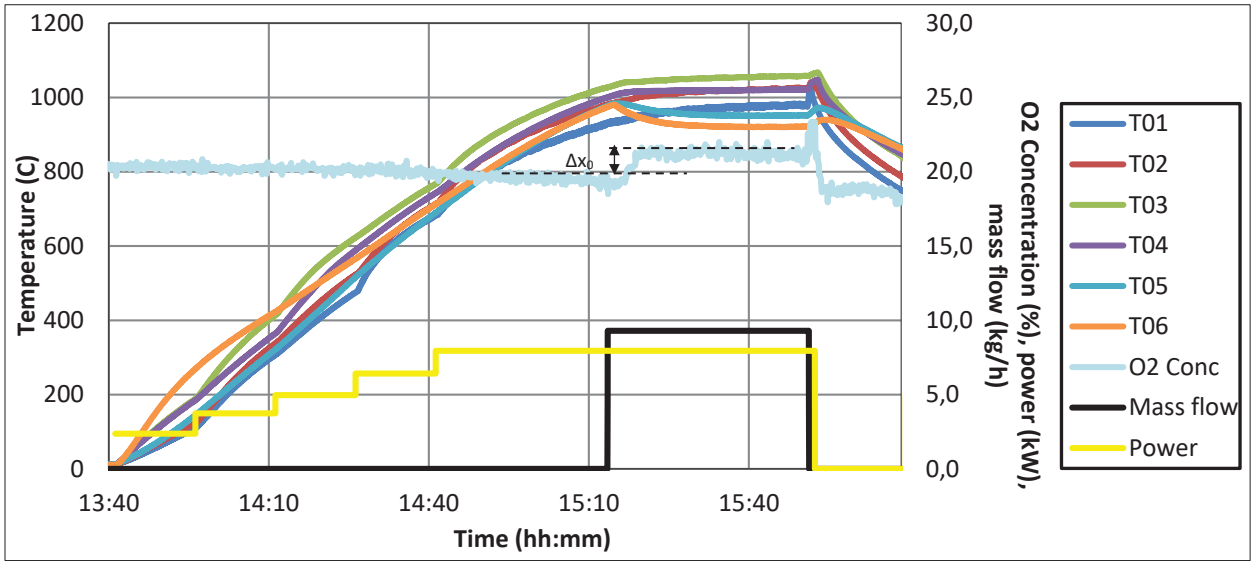

FIGURE 2. Application 1. Temperature evolution (left axis) following the colour code in of Fig. 1 a. On right axis: incident power, particle flow and oxygen concentration.

The incident power increases step-wise to avoid thermal shocks that could damage the reactor. An additional lamp of the solar simulator is switched on every 15 minutes, ramping up the power stepwise to eventually 8 kW. After 1.5 h of heating phase, a particle flow of 9.2kg/h starts. The temperatures at the back of the reactor sharply decrease due to the entrance of cooler particles from the feeder. The particles heat up at the back of the crucible reaching 1022°C in the center of the crucible, whereas the maximum temperature of 1058°C is obtained at 17.5 cm from the front. At 5cm from the front, the particles are still at 1025°C but cool down to 980°C in the last few centimetres. An area of 30 cm with temperature higher than 1000°C was obtained. Within this zone the temperature difference is less than 35°C. In the front part, the air coming from the cold storage, the higher radiation losses and the lower incident flux lead to a clear decrease in temperature. It has to be mentioned that in order to avoid material deactivation, the maximum temperature is limited to 1100°C [19, 30]. To keep the reactor below this temperature, only the six central lamps of the solar simulator are switched on. The addition of the four more peripheral lamps would increase the incident flux at the front and reduce the temperature difference.

When the particle flow starts, the oxygen concentration increases significantly, clearly indicating the reduction reaction. Through the oxygen concentration increase (Δx_{O2}, shown in Fig. 2), the reaction advancement (X) was calculated:

$$X = \frac{\dot{n}_{O2}}{\dot{n}_{O2,Max}} \quad \text{with} \quad \dot{n}_{O2} = \dot{n}_{air} \cdot \Delta x_{O2} \quad \text{and} \quad \dot{n}_{O2,Max} = \frac{1}{6}\dot{n}_{(Mn,Fe)2O3} \qquad (2)$$

Where $\dot{n}_{O2}$ is the net molar flow of oxygen (in addition to the one transported by air), $\dot{n}_{O2,Max}$ is the maximum molar flow of oxygen which can be generated by a complete reduction of the particle flow, $\dot{n}_{(Mn,Fe)2O3}$ is the molar particle flow. In the first tests, a maximum conversion of 40% was obtained. An increase in the residence time in the hot zone is likely to increase this value.

Cement Production

The second experiment with the rotary kiln concerned the cement production process. Cement production involves two energy-intensive phases: the calcination of CRM at about 1000°C and the clinkering process at about 1400°C. The objective of this study is to drive the first step through concentrated solar energy, avoiding fuel consumption for this phase. The calcined material should be stored at a high temperature and in a real plant be fed into a conventional clinkering furnace to produce cement. CRM is a mixture of $CaCO_3$ (80-85% of total mass) and other aggregates such as silica and alumina. During calcination, $CaCO_3$ undergoes the reaction:

$$CaCO_3 \rightarrow CaO + CO_2 \qquad (3)$$

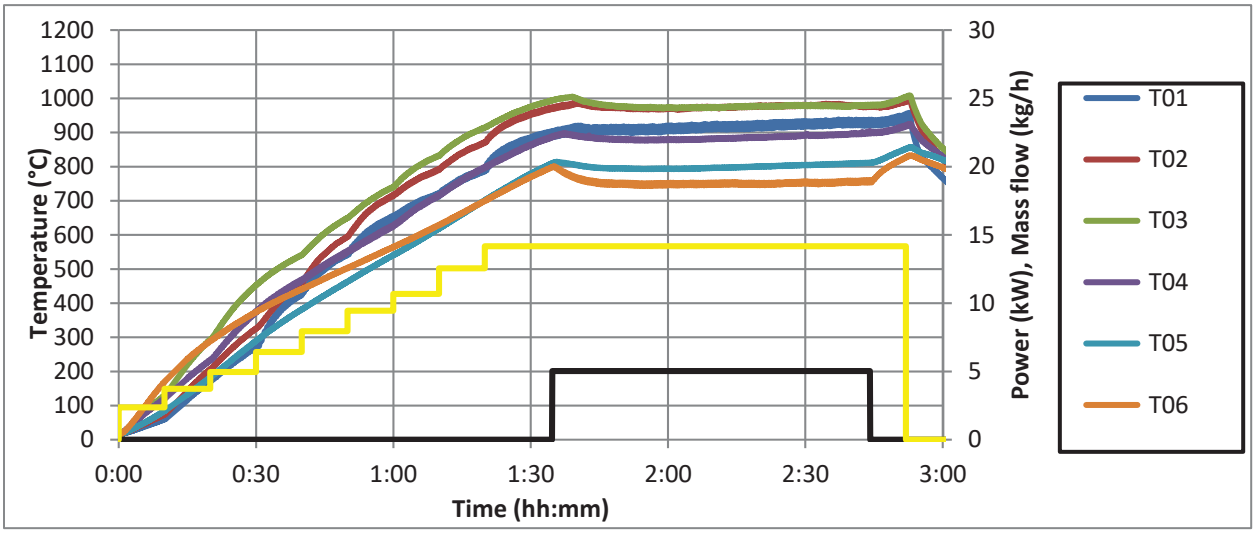

FIGURE 3. Application 2. Evolution of the temperature (left axis) according to the colour code in Fig. 1a. On the right axis: incident power, particle flow and oxygen concentration.

The particle size, between 1-176 µm, must be small enough to ensure a solid-solid reaction between CaO and the aggregates in the subsequent clinkering process.

The first tests were carried out in a closed configuration, using a quartz window at the aperture. 30 minutes after the start of feeding, dust has been deposited on the window, preventing the entry of solar radiation. In order to be able to operate for several hours without interruption, the experiments were continued in an open configuration (Fig. 1, gas outlet 2). A parallel study is analysing other options to operate in a closed configuration and thus also collect the CO_2 produced by the reaction.

Figure 3 shows exemplary results. The reactor is gradually heated for 1.5 hours, after which the particle flow started. The temperature at the back decreases abruptly to adapt to the temperature of the input material, before it stabilizes. After about 15 minutes the temperature in the entire crucible stabilizes. The temperature of the particles increases by 150°C in the back half of the reactor, reaching 890°C in the central position. The temperature increases further towards the front of the reactor, until it reaches a plateau (T02-03) at about 980°C where the chemical

reaction takes place. Once again, the particles cool down at the reactor front to 920°C. This is due to the high heat losses associated with air suction.

In this case, the conversion of the solid material can be calculated indirectly by post-operation thermogravimetric analysis (TGA) under air atmosphere where any eventual further calcination of the material can be quantified in terms of weight decrease. Such an analysis of the material leaving the reactor showed a conversion rate of 88% reached in the solar reactor.

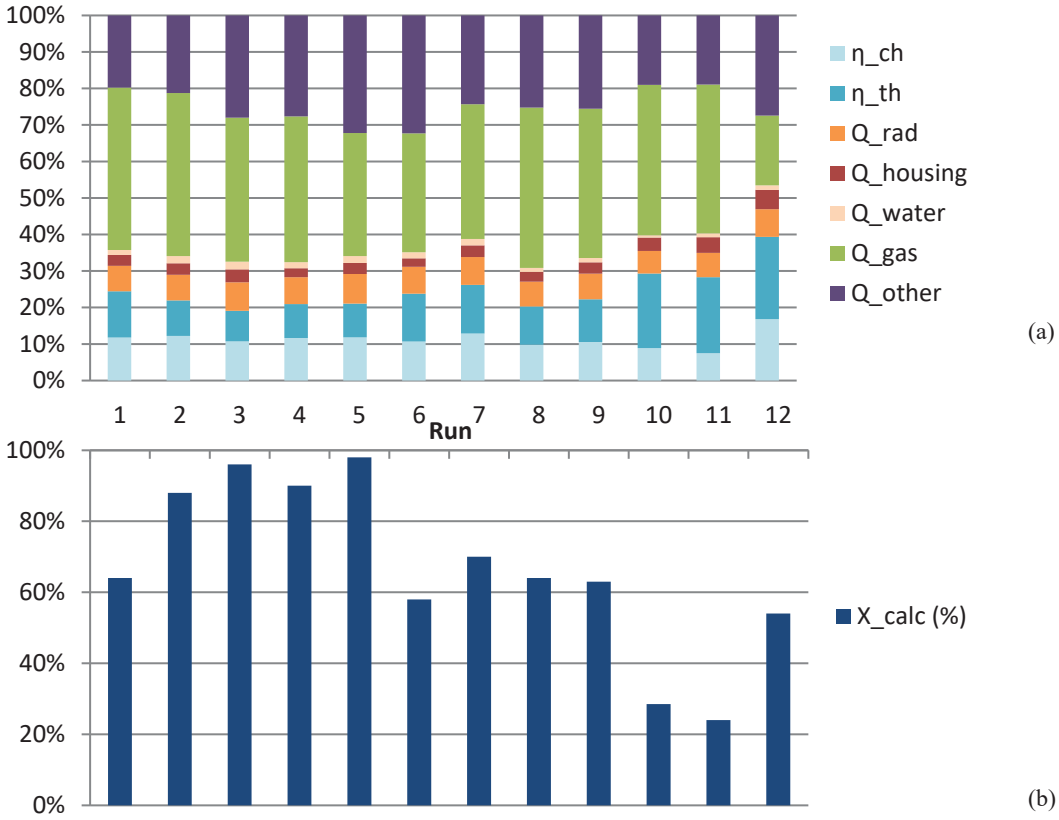

FIGURE 4. Heat losses and conversion for the complete campaign

The complete experimental campaign consisted of 13 chemical experiments. The system was able to operate for several hours and for several days continuously. Operating parameters such as temperature, mass flow and residence time were varied to optimize the process. The total (η_{Tot}) and chemical (η_{chem}) reactor efficiency is calculated as follows:

$$\eta_{Tot} = (Q_{use\_ch} + Q_{use\_th})/Q_{inc} \quad (4)$$

$$\eta_{chem} = Q_{use\_ch}/Q_{inc} \quad (5)$$

where Q_{use_ch} is the power absorbed by the material through the chemical reaction. This derives from the particle flow rate and the conversion measured through TGA. Q_{use_th} is the power absorbed by the material to reach the outlet temperature (T01), calculated through the particles mass flow and specific heat. It is interesting to note that although in thermal tests [31] an efficiency of more than 60% could be achieved, for a chemical conversion of more than 60% the total efficiency of the reactor was less than 30%. Heat losses were analysed to explain the reason for this. Figure 4 resumes the experimental campaign describing the heat losses, efficiencies, and chemical conversion for each test. The test shown in Fig. 3 corresponds to Run 2 in Fig. 4. The heat fluxes are calulated based on the measured temperature and mass flows (of particles, gas and water in the cooling system) and divided by the incident power to derive the losses. Q_rerad are the radiation losses through the reactor aperture, Q_housing are the radiation and convection through the external housing, Q_water are the losses due to the water cooling of the screw feeder,

Q_others refers to the losses that could not be quantified, such as losses from the front and rear housing plates or possible reflection of the incident radiation by the dust created inside the kiln. The detailed calculation of these losses can be found in [31]. In this study, one more loss mechanism is evaluated, i.e. Q_gas corresponding to the convectional losses due to the suction gas.

It can be seen that the radiation losses, which are expected to be predominant, are limited to 8% of the incident power. The losses through the external housing are even smaller (less than 5%) due to the effective insulation used. The cooling system absorbs less than 2% of the total radiation. The main factors contributing to the low efficiency are the convection losses through the flushing gas, which can absorb up to 45% of the incident power. This flow has probably been oversized to prevent the release of any particles. In Run 13 it can be seen how a smaller flow can reduce the convection losses (below 20%) and lead to a total efficiency of 40%.

CONCLUSIONS

In the present study, two different materials have been successfully treated to demonstrate the suitability and versatility of a solar rotary kiln: redox oxide granules of mm size have been thermally reduced to store high temperature thermochemical energy and micrometric particles of $CaCO_3$ have been calcined to produce lime (as the main ingredient of cement). The reactor has been developed and iteratively improved over several experimental campaigns, where the system has been optimized and problems have been progressively solved. In the first application, metal oxide granules of mm size are heated up to 1060°C and are chemically reduced. In this case, the reactor works in closed configuration to monitor the gas composition as an indicator of the reaction advancement. Thermal tests of the reactor exhibit a temperature gradient inside the reactor of less than 80°C between the hottest point and the particle outlet placed at the front. This gradient could be further reduced by moving the particle outlet few cm to the back. After a heating-up phase, the particle flow was initiated and the chemical reaction was clearly demonstrated by the increase in the oxygen concentration in the outlet. In the second application, the cohesive micrometric particles of CRM are heated to about 1000°C and calcined. The reactor operated in an open configuration to prevent the deposition of dust on the window. In this case, 13 chemical tests were successfully carried out. The study of the energy flows allowed to define that the main heat losses occurred by convection. This showed that gas flow is a critical factor to be optimized to improve reactor performance. A total efficiency of about 40% was achieved by reducing the gas flow. Further ongoing studies are analyzing the possibility of operating the system with the presence of a window.

ACKNOWLEDGMENTS

The authors would like to thank the European Commission, the Bundesland Nordrhein-Westfalen and the DLR ProgrammdirektionEnergie (PD-E) for partial funding of this work within the Project SOLPART –contract No 654663 under the Horizon 2020 research and innovation programme, within the Project CALyPSOL – contract No EFRE-0801159 under the European fund for regional development and EFRE.NRW Investitionen in Wachstum und Beschäftigung, and within the Project REDOXSTORE,

REFERENCES

1. F. M. Trombe F., *Bulletin de la societe chimique de france* 5eme serie, 1315-1322 (1954)
2. G. Flamant, et al., *Solar Energy* **24**, 4, 385-395 (1980)
3. K.-H. Funken, et al., *Journal of Solar Energy Engineering* **123**, 2, 117-124 (2001)
4. C. Glasmacher-Remberg, et al., *AL aluminium and its alloys* **135**, 73 - 77 (2001)
5. M. Neises-von Puttkamer, et al., R.E. Kirchain, et al., Editors. 2016, Wiley TMS: Nashville, USA. p. 235-240.
6. K.-H. Funken, et al., *Solar Energy* **65**, 1, 25-31 (1999)
7. M. S. Haueter P., Palumbo R., Steinfeld A., *Solar Energy* **67**, 161-167 (1999)
8. P. Charvin, et al., *Chemical Engineering Research and Design* **86**, 11, 1216-1222 (2008)
9. M. Neises, et al., *Solar Energy* **86**, 10, 3040-3048 (2012)
10. E. Alonso, et al., *Renewable Energy* **105**, 665-673 (2017)
11. E. Alonso, et al., *Solar Energy* **115**, 297-305 (2015)
12. A. Meier, et al., *Energy* **29**, 5–6, 811–821 (2004)
13. A. Meier, et al., *Journal of Solar Energy Engineering* **127**, 3, 386–395 (2005)

14. A. Meier, et al., *Solar Energy* **80**, 10, 1355-1362 (2006)
15. S. Tescari, et al., *AIP Conference Proceedings* 2033, 1, 130014 (2018)
16. S. Breuer, et al., "*Thermochemical solar energy storage via redox oxides: development of a continuous rotary kiln reactor for redox reactions with cobalt oxide*", in *14th International Conference on Clean Energy (ICCE-2014)*. 2014. Istanbul, Türkei: 14th International Conference on Clean Energy (ICCE-2014).
17. G. Dibowski, et al., "*Der neue Hochleistungsstrahler des DLR - Grundlagen, Technik, Anwendung*", in *10. Kölner Sonnenkolloquium 2007*. 2007. Köln: DLR e.V. - Institute of Solar Research.
18. P. Pardo, et al., *Renewable and Sustainable Energy Reviews* **32**, 591-610 (2014)
19. T. Block and M. Schmücker, *Solar Energy* **126**, 195-207 (2016)
20. C. Agrafiotis, et al., *Solar Energy* **139**, 695-710 (2016)
21. C. Sattler, et al., 2015: Boston, MA, USA.
22. G. Karagiannakis, et al., *Solar Energy* **133**, 394-407 (2016)
23. C. Pagkoura, et al., "*Co3O4-based honeycombs as compact redox reactors/heat exchangers for thermochemical storage in the next generation CSP plants*", in *SOLARPACES 2015: International Conference on Concentrating Solar Power and Chemical Energy Systems*. 2016. AIP Publishing.
24. S. Tescari, et al., *Applied Energy* **189**, 66-75 (2017)
25. M. Wokon, et al., "*Thermochemical Energy Storage based on the Reversible Reaction of Metal Oxides*", in *3rd International Conference on Chemical Looping, September 9-11*. 2014. Göteborg, Sweden.
26. A. J. Carrillo, et al., *ChemSusChem* **8**, 11, 1947-1954 (2015)
27. M. Wokon, et al., *Solar Energy* **153**, 471-485 (2017)
28. N. C. Preisner, et al., "*A Moving Bed Reactor For Continuous Heat Extraction From Metal Oxides As Thermochemical Energy Storage*", in *12th International Storage Conference on Renewable Energies (IRES) and ENERGY STORAGE EUROPE Conference*. 2018. Düsseldorf, Germany.
29. R. Buck, et al., "*Techno-economic analysis of thermochemical storage for CSP systems*", in *SolarPACES 2019*. 2019. Daegu, South Korea.
30. C. Agrafiotis, et al., *Solar Energy* **149**, 227-244 (2017)
31. G. Moumin, et al., *Solar Energy* **182**, 480-490 (2019)